Indian Journal of Chemistry
Vol. 51A, March 2012, pp. 411-419

Photocatalytic reduction of carbon dioxide by water on titania: Role of photophysical and structural properties

K Rajalakshmi, V Jeyalakshmi, K R Krishnamurthy & B Viswanathan*

National Centre for Catalysis Research (NCCR), Indian Institute of Technology Madras, Chennai 600 036, Tamil Nadu, India
Email: bvnathan@iitm.ac.in

Received 1 November 2011; revised and accepted 13 January 2012

Photocatalytic reduction of carbon dioxide has been investigated on three different titania catalysts (two commercial titania, De Gussa P-25 and UV-100 Hombikat and another catalyst prepared by sol-gel method under reverse micelle environment) dispersed in aqueous alkaline medium under irradiation in visible region (300-700 nm) from Hg lamp. The catalysts have been characterized by XRD, diffuse reflectance and fluorescence spectroscopic techniques and textural analysis. Methane, methanol and ethanol are observed as the major products. Activity in terms of total hydrocarbons production and (methane + methanol) yields during six hours run follows the order: P-25>RM-TiO_2>UV-100. Ethanol is formed in significant amounts in the case of UV-100 and RM-TiO_2 but not with P-25. Probable reaction pathways that lead to the formation of these products have been proposed. While the catalytic activity is governed by the generation and life span of photo-induced charge carriers, it is envisaged that product selectivity is determined by the type of transformations that the transient surface species undergo on titania. Surface Ti ions with singly or doubly vacant coordination sites (four or five coordinate Ti ions) act as active centres for these transformations. The relative population of four/five coordinate Ti ions play a vital role in directing the transformations and hence selectivity. The coordination environment of surface Ti atoms evolves during catalyst preparation. Photophysical as well as structural properties of titania samples influence their overall catalyst performance.

Keywords: Photocatalytic reduction, Photophysical properties, Titania, Carbon dioxide reduction, Structural properties

Photocatalytic reduction of carbon dioxide with water on semiconductor oxide catalyst surfaces using solar energy to yield fuels/chemicals (methane, methanol, etc.) has the potential to become a viable and sustainable alternative energy source to fossil fuels[1-3]. The process involves two major steps, splitting of water to yield hydrogen, which in turn helps in the reduction of carbon dioxide to different hydrocarbon products in the second step. Design of effective catalysts for such a complex process, involving multi-electron transfer steps, holds the key for the viability of the process.

Ideal catalysts are expected to display maximum efficiency towards solar energy absorption and possess requisite band energy level characteristics to drive the redox reactions on the semi-conducting catalyst surface. Functionally, the catalysts should have valence band top energy level suitable for splitting of water to generate hydrogen, which is the primary step. The second and the crucial step is the reduction of CO_2 to hydrocarbons, which requires the bottom energy level of the conduction band to be more negative with respect to reduction potential for CO_2. It is essential that the photo-generated electrons and holes are spatially separated so that they have sufficient life time to initiate redox reactions on titania surface. In this respect, the life time of the photogenerated electrons is a crucial factor for the photo-reduction of water as well as CO_2. The complex sequence of process steps that follow, involving two, four, six or eight electrons for reduction, lead to the formation of formic acid/CO, formaldehyde, methanol and methane respectively[4,5], depending on the type of catalyst and reaction conditions employed.

Titania in various crystalline, morphological and nanostructural (tubes, sheets, films, foams etc.) forms modified by doping with metals and anions, titania coupled with various semiconductor oxides and binary/ternary oxides of titanium with oxides of tantalum, niobium, alkaline earth and rare earth, has been extensively studied as catalysts[1-6]. Intrinsic properties of titania, like, particle/crystallite size, phase composition (anatase and rutile), surface area, surface hydroxyls, lattice defects and the type and level of dopants (metals and non-metals) influence its performance[1-6]. Photocatalytic activity and phase

transition behavior of TiO_2 are significantly influenced by the preparative conditions and methods[7-10].

One of the most interesting aspects of photocatalysis by titania (for air and water purification, hydrogen generation from water and reduction of CO_2 by water) is the effect of its phase composition, mainly anatase and rutile contents, in a given titania sample. Divergent views prevail on the activity of mixed phases of titania and the scientific reasons therein. A number of studies[11-15] conclude that a mixed phase titania with specific composition (of anatase and rutile) is more active than pure anatase or rutile, since the synergy between the phases[15] is said to be beneficial in reducing the recombination of photogenerated electrons and holes, thereby increasing their life time and utility. According to Hurum *et al.*[16], mixed-phase titania catalysts show higher activity due to three factors: (1) the smaller band gap of rutile extends the useful range of photoactivity into the visible region, (2) the stabilization of charge separation by electron transfer from rutile to anatase slows recombination, and (3) the small size of the rutile crystallites facilitates this transfer, making catalytic hot spots at the rutile/anatase interface.

Chen *et al.*[17] carried out photocatalytic reduction of CO_2 with water on a series of sputtered mixed phase titania films and observed that the film with the composition of 70% anatase, 30% rutile proved to be far superior to the other compositions towards methane formation. Similarly, Li *et al*.[18] have confirmed the positive synergy effect in mixed phase titania nanocomposites prepared by hydrothermal method for photo-oxidation of methylene blue as well as photoreduction of CO_2. However, Ohtani *et al.*[19], on the basis of their studies involving separation and characterization of anatase and rutile phases from P-25 and reconstruction of P-25 phase, concluded that there is no such synergy effect for a set of reactions studied.

Besides the life of the charge carriers, the concentration of surface hydroxyl groups and hence the crystallite form and surface area of the titania also play a vital role as reported by Carniero *et al.*[20-22] for selective photo-oxidation of cyclohexane, wherein the reaction medium, aqueous or non-aqueous, also influences the activity.

Xia *et al.*[23] in the course of their studies on photocatalytic reduction of CO_2 with water on titania-multi-walled carbon nano tubes (MWCNT) composites observed that the product profile/selectivity depends on the method of preparation of titania. While the titania prepared by sol-gel route (mainly anatase) displays higher selectivity towards ethanol, that prepared via hydrothermal route (rutile phase) selectively yields formic acid.

Selectivity/product profile is also governed by the wavelength of the radiation used. Besides the band–gap excitation, sub-band gap excitations (due to lattice defects) and formation of charge transfer complexes with the reactants may affect the activity and the product selectivity as observed in the case of 2,4,5-trichlorophenol conversion on P-25, leading to wavelength dependent reaction paths[24]. Thus, a clear picture of the role of intrinsic photo-physical and structural properties of titania in governing the activity and selectivity for photocatalytic reactions in general, and specifically for reduction of CO_2 with water, is yet to emerge.

In this context, we have carried out investigations on photocatalytic reduction of CO_2 with water on three titania samples (P-25, Hombikat-UV-100 and RM-TiO_2) and attempted rationalization of the observed activity/selectivity patterns in terms of their photophysical and structural characteristics and the probable mechanistic pathways.

Materials and Methods

Preparation of catalysts

Commercial samples, P-25 (DeGussa) and Hombikat-UV 100 (Sachtleben Chemie GmbH) were used as such. RM-TiO_2 was prepared by sol-gel method[25], by slow drop-wise addition of titanium (IV) iso-propoxide into the hydrolysis medium consisting of cyclohexane, anionic surfactant-Triton-X-114 and distilled water, with vigorous stirring, under reverse micelle environment and ambient temperature. Molar ratio of cyclohexane: Triton:water:titanium iso-propoxide was 11:1:1:1. The sol was stabilized for 15 minutes and then allowed to gel at ambient temperature for 24 hrs, followed by calcination in air at 400 °C for 4 hours to obtain RM-TiO_2.

Characterization of catalysts

The crystal phase of the catalysts was analyzed by X-ray diffractometer (Rigaku-MiniFlex-II) using CuK_α radiation (λ = 1.54056 Å) in the scan range of 2θ = 5-90° at a speed of 3°/min.. Crystallite sizes were calculated by Scherrer's formula, $t = K\lambda/\beta \cos\theta$, where t is the crystallite size, K is the constant

dependent on crystallite shape (0.9 for this case); λ = 1.54056 Å, β is the FWHM (full width at half maximum) and θ is the Bragg's angle.

The phase composition of TiO2 was analyzed using the relative peak intensity of anatase and rutile[26], $F_A = 1/[1+ 1.26 (I_R/I_A)]$, where F_A is the fraction of anatase phase and I_R and I_A are the intensities of peaks due to rutile and anatase phases respectively.

Diffuse reflectance absorption spectra of the catalysts in the UV-visible region were recorded using a Thermo Scientific Evolution 600 spectrophotometer equipped with a Praying Mantis diffuse reflectance accessory. The fluorescence spectra of catalysts were measured by a JY Fluorolog-3-11 spectrophotometer at an excitation wavelength of 260 nm. Surface area and pore volume of the catalysts were measured using Micromeritics ASAP 2020. Samples were degassed at 373 K for 2 h and at 423 K for 3 h. Pure nitrogen at liquid nitrogen temperature (77 K) was used.

Photocatalytic reaction

The photocatalytic reactor as shown in Fig. 1 was used to follow the reduction of CO_2 by water under radiation in UV-visble range 300-700 nm from a 250 W high pressure Hg lamp. A jacketed all-glass reactor (620 mL) fitted with quartz window (5 cm dia.) was filled with 400 mL of aqueous 0.2 *N* NaOH solution and 0.4 g of the catalyst was dispersed in the medium by vigorous stirring. Aqueous alkaline solution (at *p*H-13.0) was then saturated with pure CO_2 by continuous bubbling for 30 minutes after which the *p*H turned 8.0. Reactor inlet and outlet valves were then closed and irradiation with Hg lamp with 77 W power (from WACOM HX-500 lamp house) was started. After every two hours, gas samples were taken out with a 500 µl gas-tight syringe and analysed by gas chromatography (Perkin Elmer, Clarus 580 GC, Poroplot Q column and FID).

Blank experiments (reaction with irradiation without catalyst and reaction in dark with catalyst) were conducted to ensure that the product formed was due to the photoreduction of CO_2. No product in measurable quantities could be detected in liquid samples. The high rate of stirring (400 rpm) maintained to ensure good dispersion/suspension of titania in solution perhaps allows the products to escape into gas phase.

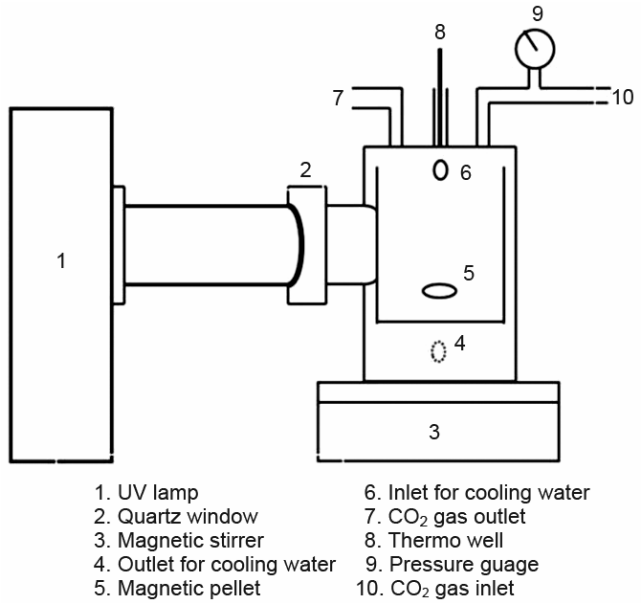

Fig. 1—Experimental setup for photocatalytic reduction of CO_2 by water.

Results & Discussion

Characterization of catalysts

X-ray diffraction patterns of the prepared and commercial samples are given in Fig. 2. XRD peaks at 2θ = 25.28°, 37.98°, 48.38°, 53.98°, 55.08°, 62.78°, 68.98°, 70.18° and 75.58° were identified as due to anatase phase, and those at 2θ = 27.58°, 36.18°, 41.38° and 48.18° represented rutile phase (JCPDS data 89-4920 and 89-4921). Hombikat-UV-100 and RM-TiO_2 contain pure anatase phase, while P-25 consists of 85 % anatase and the rest rutile.

Diffuse reflectance spectra of the titania samples in UV-visible region are presented in Fig. 3 and the

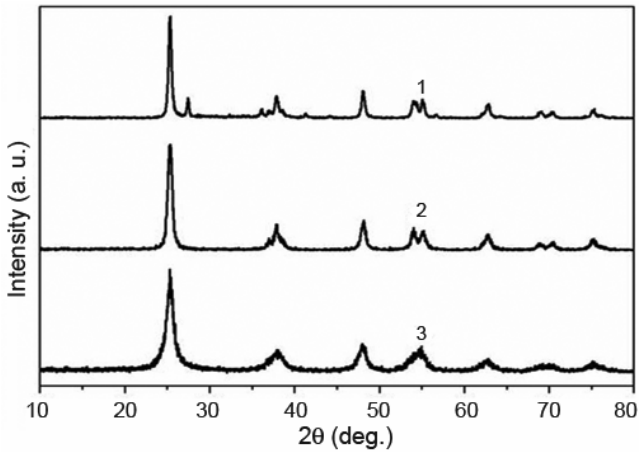

Fig. 2—XRD patterns for titania catalysts. [1, P25; 2, RM TiO_2; 3, Hombikat].

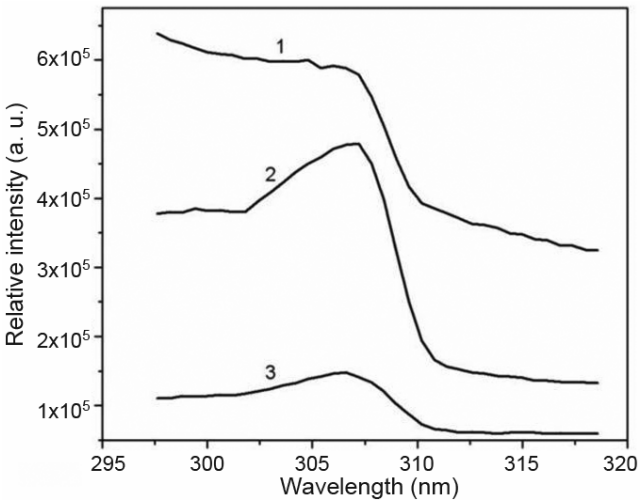

Fig. 3—Fluorescence spectra of titania catalysts. [1, RM TiO_2; 2, Hombikat; 3, P25].

Table 1—Physico-chemical characteristics of the catalysts

Sample	Phase comp. (%)	Surface area (m^2/g)	Crystal size (nm)	Band gap (eV)
P-25	Anatase (85) Rutile (15)	50	22	3.02
Hombikat UV-100	Anatase	311	9	3.04
RM-TiO_2	Anatase	48	12	3.06

band gap values measured as per standard procedure are given in Table 1 along with other characteristics. P-25 displays the lowest band gap value due to the presence of rutile phase in measurable proportions.

Significant variations however, are observed in the fluorescence spectra of the samples (Fig. 3). Lower fluorescence intensity for P-25 is due to the reduced number of recombination sites resulting in longer life-time of photoelectrons on the TiO2 surface, thus leading to a higher photocatalytic activity. The reduction in recombination in P-25 is due to the co-existing rutile phase, whose valence band and conduction band levels are slightly higher than those for anatase[15,16]. At the anatase-rutile interface, such energy levels promote charge separation, thereby reducing fluorescence intensity. Both Hombikat UV-100 & RM-TiO_2 display intense fluorescence indicating higher charge recombination rates.

Photocatalytic activity

The effects of such changes in the photophysical properties are clearly seen in the activity pattern for CO_2 conversion, P-25> RMTiO_2> Hombikat (Table 2). Activity is expressed as micromoles of CO_2 consumed in six hours, which is calculated as per the stoichiometry. Methane and methanol are the major products formed on all the three samples. Ethanol is observed on Hombikat and RM-TiO_2 but surprisingly not on P-25, the most active amongst the three. With UV radiation (365 nm), Xia *et al.*[23] observed methane and formic acid as major products on (P-25 + MWCNT) composite, with very little ethanol (~ 5 micro moles/g) but no methanol. Formation of ethanol on TiO_2 (anatase) has been observed earlier by Mizuno *et al.*[27], but at higher pressures of CO_2. Subrahmanyam *et al.*[28] have reported that on acidic titania composites only C_1 hydrocarbons are formed, while on composites with basic character, C_1-C_3 hydrocarbons including ethanol are observed. Thus, the basic characteristics of titania could be one of the factors responsible for formation of C_2 hydrocarbons like ethanol/acetaldehyde, etc. It is also known that titania contains both acidic as well as basic sites and its reduction with the formation of Ti^{3+} generates basic sites[29].

Table 2—Photocatalytic reduction of CO_2 by H_2O

Catalyst	Yield[a] (μmol/g)			Total CO_2 consumed
	CH_4	CH_3OH	C_2H_5OH	
P25	0.7	914	0	915
Hombikat UV-100	0.3	118	53	216
RM TiO_2	0.6	130	59	249

[a]Yields after 6 h of irradiation.

Activity versus photophysical properties

The major factors responsible for the higher activity observed for P-25 in the present case are the stabilization of charge separation as evidenced by the low intensity fluorescence spectrum and the existence of positive synergy effect between anatase and rutile phases, which has been substantiated by earlier work[11-16]. Both Hombikat-UV-100 and RM-TiO_2 with higher charge recombination rates display relatively lower activity, their lower particle sizes leading to an increase in the density of recombination centres[25]. Trends observed in methane formation, which requires the maximum photogenerated electrons population for eight electrons transfer, are also in tune with this concept. Besides, Hombikat titania which is the least active, is known to adsorb water strongly[30], which may adversely affect the adsorption/activation of CO_2/HCO_3^- and hence the overall activity.

An interesting observation in the present work is the product profile, especially for methanol and ethanol formation. Maximum methanol formation is observed with P-25, which surprisingly does not form ethanol in measurable quantities, while it is formed in substantial amounts on RM-TiO_2 and Hombikat, which are relatively less active for overall CO_2 conversion.

Xia *et al.*[23], who studied CO_2 photoreduction on various titania-MWCNT composites, observed methane, formic acid and ethanol as major products, but not methanol. Possibly, the nature of nanocarbon support, phase composition (anatase/rutile) of titania and the wavelength of radiation used (365 nm) could be responsible for driving the reaction along the specific path. Though ethanol formation has been observed earlier[31] on AgBr/P-25 with visible light at 420 nm in 0.2 *M* $KHCO_3$ solution saturated with CO_2, the elementary steps leading to its formation are not clear. An understanding of the elementary reaction steps is therefore needed to explain the observed product profile for three titania samples.

Reaction pathways

The first step involving photocatalytic splitting of water follows the well-accepted elementary steps as shown in Eqs (1) to (6):

$$TiO_2 + h\nu \longrightarrow e^- + h^+ \quad ...(1)$$

$$H_2O \longrightarrow H^+ + OH^- \quad ...(2)$$

$$H^+ + e^- \longrightarrow H. \quad ...(3)$$

$$OH^- + h^+ \longrightarrow OH. \quad ...(4)$$

$$2\ OH. \longrightarrow H_2O_2 + h^+ \longrightarrow O_2^- + 2H^+ \quad ...(5)$$

$$O_2^- + h^+ \longrightarrow O_2 \quad ...(6)$$

The second step for activation and reduction of CO_2 could then follow different pathways. Anpo *et al.*[32] have identified ESR signals due to C and H atoms, CH_3 radicals and Ti^{3+} ions on powdered titania catalysts in presence of CO_2 and water at 77 K. Accordingly, the following pathway (Mechanism A) involving the formation of active surface carbon and its reaction with H and OH radicals, have been proposed by Anpo *et al.*

Observations by Yang *et al.*[33] on the formation of carbon residues and ESR evidence on hydrogen, methyl and methoxy radicals and CO_3^- anion radicals by Dimitrijevic *et al.*[34] on titania surface during CO_2 photoreduction lend credence to this mechanism. Besides, CO as one of the reduction products has been reported on titania and metal supported titania[35].

A different route (Mechanism B, Fig. 4) involving HCOOH as the primary intermediate has been proposed by Wu[36] based on *in situ* IR spectroscopic studies. IR absorption bands due to bicarbonate, carbonate, formate, formaldehyde and methoxy species on TiO_2 surface have been observed. Accordingly, methanol is formed through surface methoxy species and its further reduction results in methane formation.

Similar reaction pathway have been proposed earlier by Subrahmanyam *et al.*[28] for mixed oxides of titania and by Sasirekha *et al.*[37] for Ru supported on TiO_2 dispersed on SiO_2. Formation of methane via methanol seems to be unlikely, since added methanol does not lead to increase in methane formation[38]. Kinetic equations[39,40] based on Mechanism A, developed for photoreduction of CO_2 with water on

Mechanism A

$$CO_2 + e^- \longrightarrow .CO_2^- \quad ...(7)$$

$$.CO_2^- + .H \longrightarrow CO + OH^- \quad ...(8)$$

$$CO + e^- \longrightarrow CO^- \quad ...(9)$$

$$.CO^- + .H \longrightarrow .C + OH^- \quad ...(10)$$

$$.C + H^+ + e^- \longrightarrow .CH \rightarrow .CH_2 \rightarrow .CH_3 \quad ...(11)$$

$$.CH_3 + H^+ + e^- \longrightarrow CH_4 \quad ...(12)$$

$$.CH_3 + .OH \longrightarrow CH_3OH \quad ...(13)$$

Mechanism B

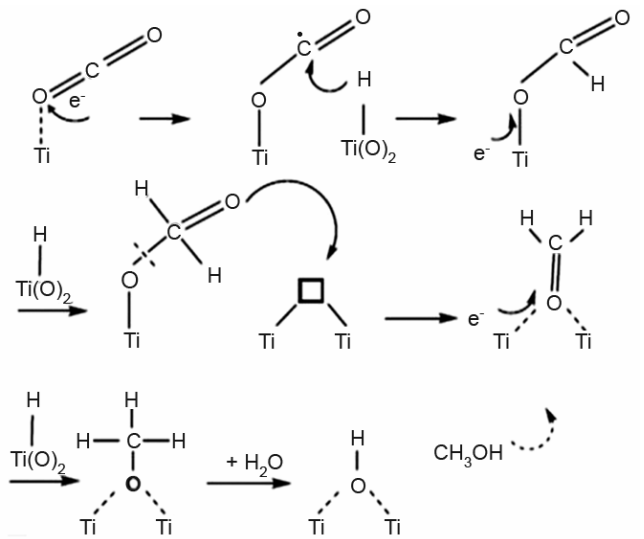

Fig. 4—Reaction pathway for photocatalytic reduction of CO_2 by water on TiO_2 (Mechanism B).

TiO_2, could be validated with the experimental data indicating that it has better acceptability than Mechanism B.

In the present work, major products observed are methane, methanol and ethanol. Methyl radical could be the common intermediate in the formation of methane/methanol. Population and lifetime of photogenerated electrons are the critical factors responsible for the formation of methane. In the present investigation, with aqueous alkali as the medium, the availability of surface hydroxyls and **.**OH radicals are responsible for methanol formation.

Ethanol formation by CO_2 photoreduction on titania/titania based catalysts has been observed earlier[23,27,28,41], though the pathway leading to its formation is yet to be understood. Liu *et al.*[42] have reported selective ethanol formation on monoclinic $BiVO_4$, a photocatalyst for O_2 production from water and proposed dimerization of surface C_1 species as the route for ethanol formation. Formation of ethanol may be envisaged to proceed through coupling of ethyl and methylene radicals as shown below:

$$\cdot CH_3 + \cdot CH_2 + e^- \longrightarrow CH_3\text{-}CH_2 + \cdot OH \longrightarrow CH_3\text{-}CH_2\text{-}OH \quad ...(14)$$

Such a pathway is in line with routes proposed for formation of ethylene and ethane via dimerization as observed on Cu/TiO_2 and TiO_2 and ZrO_2 respectively[43,44].

$$\dot{C}H_3 + \dot{C}H_3 \longrightarrow CH_3\text{-}CH_3 \quad \ldots(15)$$

$$\dot{C}H_2 + \dot{C}H_2 + 2e \longrightarrow CH_2{=}CH_2 \quad \ldots(16)$$

Surface structural features of titania that facilitate such transformations are discussed later in this article.

Since Mechanism A involves CO as one of the intermediates, in presence of H_2 photocatalytic Fischer-Tropsch route to > C_1 hydrocarbons that proceed through surface carbides could be another pathway[45]. In particular, when the reaction is carried out under pressure so as to improve the limited solubility of CO and H_2 in water, such transformations are possible. Mizuno *et al.*[27] did observe formation of > C_1 hydrocarbons and ethanol during CO_2 photoreduction at higher pressures using TiO_2 dispersed in aqueous alkaline solution. It is then essential that the crystal structure of titania with appropriate sites should facilitate bimolecular surface reactions envisaged above.

Influence of structural properties of titania

Surface density and the coordination environment of individual Ti^{4+} ions are the two key parameters that govern the reactivity. Influence of surface structure of titania on activity and selectivity during CO_2 photoreduction was observed by Anpo *et al.*[32] in their studies on $TiO_2(100)$ and $TiO_2(110)$ surfaces. Overall CO_2 conversion was high on TiO_2 (100) surface with the formation of both methane and methanol (3.5 and 2.4 nanomoles/h/g cat respectively) while lower conversion with only methanol (0.8 nanomoles/hr/g cat) was observed on $TiO_2(110)$ surface. Higher atomic [Ti]/[O] ratio (proportional to the number of active sites) on $TiO_2(100)$ surface is suggested as the basis for the increase in activity.

Surface cation (Ti^{4+}) density that influences the overall activity varies significantly in anatase and rutile phases. For low index planes like (101), cation density is 5.2 versus 7.9 Ti atoms/nm^2 and for (100) it is 2.8 versus 7.4 Ti atoms/nm^2 for anatase and rutile respectively [46, 47]. Effect of this factor is observed in the proportionately higher aliphatic alcohols uptake by polycrystalline rutile vis-à-vis anatase[48]. Thus, higher density of surface Ti atoms in rutile, which constitutes ~15–20 % in a typical P-25 phase, could be an additional factor contributing towards its higher activity, though moderated by easy charge re-combination. In the case of pure rutile phase however, shorter life cycle of charge carriers due to facile recombination, coupled with the presence of fewer surface hydroxyl groups relative to anatase, renders it less reactive.

Evidence for the presence of four and five coordinated surface Ti^{4+} ion sites emerges from the *in situ* IR spectroscopic studies on adsorption of water and CO_2[49] and adsorption and decomposition of primary alcohols (C_1-C_3)[48] on polycrystalline anatase and rutile surfaces. In the case of anatase,[49] two types of chemisorbed –OH species (corresponding to 3676 cm^{-1} on (001) plane and 3716 cm^{-1} on (100) and/or (010) plane) and two types of molecularly adsorbed water (3694 and 3495 cm^{-1} on (100) 3660 and 3465 cm^{-1} on (010) planes) have been observed by Tanake and White[49]. While four coordinate Ti^{4+} ions act as sites for both molecularly adsorbed water and –OH groups, the five coordinate Ti^{4+} sites adsorb –OH only. CO_2 forms bidentate carbonate and bicarbonate species on titania surface.

According to Lusvardi *et al.*[48] at room temperature, C_1-C_3 aliphatic alcohols get adsorbed in molecular and dissociated forms, a behavior similar to that of water. On dissociation, alcohols form alkoxides and hydroxyls on the surface. The behavior of adsorbed species is then governed by the coordination environment of surface Ti^{4+} ions. On heating up to 400 K the surface species recombine and desorb as alcohols, while at higher temperatures several decomposition products of alkoxides, like ethers, olefins and paraffins, aldehydes and ketones (C_1-C_3) are formed through complex surface transformations[46-48,50] involving dehydration and dehydrogenation on five coordinated Ti ions and bimolecular coupling/dimerization of surface species adsorbed on adjacent sites linked to four coordinated Ti ions. Similar observations have been made earlier[50,51] on TiO_2 single crystals. With {114} faceted (001) surface, which exposes four, five and six coordinated Ti cations, methanol desorbs as dimethyl ether, formed, while coupling of adjacent methoxy species bound to four coordinated Ti cations. On {011} faceted (001) surface which exposes five or six coordinated Ti ions, methane with highest selectivity is formed, while ether formation is not observed. Similar dependence on the local cation environment was observed with carboxylic acids as well[52] with {114} faceted (001) surface (Ti ions exposed in four and five coordination) yielding formaldehyde by coupling of formic acid. This was not observed on {011} faceted (001) surface (Ti ions exposed in five and six coordination).

On similar grounds, water gets adsorbed molecularly on (100) and (101) surfaces of rutile, and dissociatively on (110) surface[53], which can readily accommodate two–OH groups on adjacent sites linked to surface Ti ion. Water adsorption on anatase is expected to follow the same trend. Such microstructural features of titania could have a direct bearing on photocatalytic water splitting, and adsorption of CO_2 and the surface transformations that follow during CO_2 photoreduction with water. The adsorbed water promotes the formation of bidentate carbonate/bicarbonate on titania[49].

Within a reasonable degree of agreement, the transformations of alkoxide and hydroxyl species formed on titania surfaces due to adsorption of alcohols, could be compared with the possible transformations that the adsorbed methylene, methyl, methoxy and hydroxyl and species[32-34] may undergo during photoreduction of CO_2, although the process conditions/temperatures are different. CO_2 photoreduction proceeds at room temperature and hence at very low rates. The probable surface transformations[46,48] on four and five coordinated Ti ion sites are discussed below.

Scheme 1 presents the transformations on five coordinated Ti ion site, wherein the methane and/or methanol could be formed from methyl radical along with ethane, to a limited extent, by dimerization.

On four coordinated Ti ion sites, methylene and methyl radicals on adjacent sites could couple to form ethyl radical which gets transformed to ethanol (Scheme 2). Another possibility is the coupling of two adjacent methoxy species or methoxy and methyl species to form dimethyl ether, which can undergo further transformation [55] to methane and formaldehyde (Scheme 3).

Thus, the local environment of surface Ti could play a key role in controlling the selectivity of the products. These proposals, yet to be substantiated by experimental observations, provide valuable clues/leads towards understanding and establishing the actual reaction mechanism in the light of the fact that a comprehensive mechanistic path for CO_2 photoreduction is yet to emerge[54].

In short, while the energy values of the occupied and unoccupied states of semiconductor show the possibility of photo-assisted process, molecular level sites on solid surface that are responsible for the activation of the reactants denote the feasibility of the reaction in the desired direction.

It is well known that the evolution of such micro-environments on titania surface takes place during the catalyst preparation and thermal

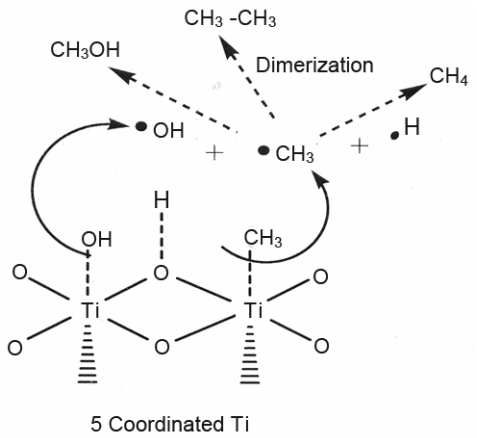

Formation of methane, methanol and ethane

Scheme 1

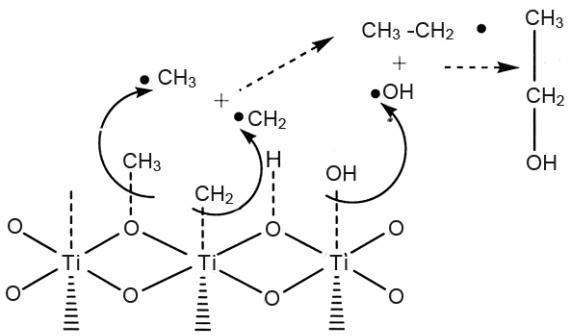

Scheme 2

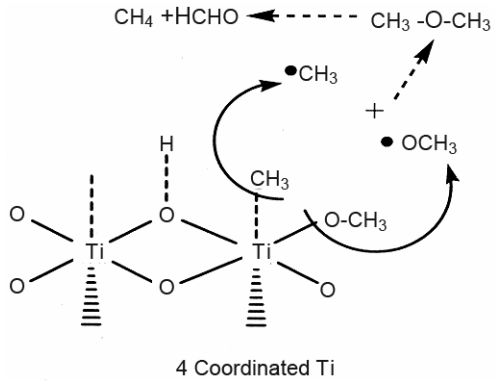

Scheme 3

pre-treatment steps. Formation of ethanol in significant quantities in RM and Hombikat titania vis-à-vis P-25 could therefore be traced to the specific procedures adopted for preparation that affect the coordination structure of surface Ti ions (relative population of four/five coordinated), and hence, the product selectivity.

Conclusions

Three different titania samples (P-25, Hombikat-UV-100 and RM-TiO_2) have been evaluated for photophysical properties and the activity for photoreduction of CO_2 with water. Methane, methanol and ethanol are the major products observed. In terms of total hydrocarbons production, P-25 displays maximum activity and yields maximum methane and methanol during six-hour run. Ethanol is formed in significant amounts in the case of Hombikat and RM-TiO_2 but not with P-25. Probable reaction pathways for the products have been proposed. While the photocatalytic activity is governed by the generation and life span of photo-induced charge carriers, it is envisaged that product selectivity is determined by the coordination environment of surface Ti ions (four/five coordinated), which in turn evolve during catalyst preparation. Photophysical as well as structural properties influence the overall catalyst performance.

Acknowledgement

Authors gratefully acknowledge the Department of Science & Technology, Govt. of India, New Delhi, for the grant towards establishing NCCR at IIT Madras, M/s Hindustan Petroleum Corporation Limited, Mumbai for a funding the project on photocatalytic conversion of CO_2 and M/s Sachtleben Chemie GmbH, Germany for samples of Hombikat-UV-100 for research studies.

References

1 Roy S C, Varghese O K, Paulose M & Grimes C A, *ACS Nano Lett*, 4 (2010) 1259.
2 Indrakanti V P, Kubicki J D & Schobert H H, *Energy Environ Sci,* 2 (2009) 745.
3 Jiang Z, Xiao T, Kuznetsov V L & Edwards P P, *Phil Trans Royal Soc A,* 368 (2010) 3343.
4 Inoue T, Fujishima A, Konishi S & Honda K, *Nature,* 277 (1979) 637.
5 Scibioh M A & Viswanathan B, *Proc Indian Nat Sci Acad,* 70A (2004) 407.
6 Koci K, Obalova L & Lancy Z, *Chem Papers*, 62 (2008) 1.
7 Kumar K N P, Keizer K, Burggraaf A J, Okubo T, Nagamoto H & Morooka S, *Nature,* 358 (1992) 48.
8 Gopal M, Moberly Chan W J & De Jonghe L C, *J Mater Sci,* 32 (1997) 6001.
9 Ito S, Inoue S, Kawada H, Hara M, Iwasaki M & Tada H, *J Colloid Interf Sci*, 216 (1999) 59.
10 Terabe K, Kato K, Miyazaki H, Yamaguchi S, Imai A & Iguchi Y, *J Mater Sci*, 29 (1994) 1617.
11 Yu J C, Yu J, Ho W & Zhang L, *Chem Comm,* (2001) 1942.
12 Bacsa R R & Kiwi, *J Appl Catal* B: *Environ,* 16 (1998) 19.
13 Yu J C, Lin J & Kwok R W, *J Photochem Photobiol A Chem,* 111 (1997) 199.
14 Ohno T, Tokieda K, Higashida S & Matsumura M, *Appl Catal A Gen,* 244 (2003) 383.
15 Yan M, Chen F, Zhang J & Anpo M, *J Phys Chem B,* 109 (2005) 8673.
16 Hurum D C, Agrios A G, Gray K A, Rajh T & Thurnauer M C, *J Phys Chem* B, 107 (2003) 4545.
17 Le Chen, Graham M E, Li G, Gentner D R, Dimitrijevic N M & Gray K A, *Thin Solid Films,* (2009), doi:10.1016/ j.tsf.2009.02.07.
18 Li G, Ciston S, Saponjic Z V, Le Chen, Dimitrijevic N M, Rajh T & Gray K A, *J Catal*, 253 (2008) 105.
19 Ohtan B, Prieto-Mahaney O O, Li D & Abe R, *J Photochem Photobiol A: Chem,* 216 (2010) 179.
20 Carneiro J T, Savenije T J & Mul G, *Phys Chem Chem Phys*, 11 (2009) 2708.
21 Carneiro J T, Yang C C, Moma J A, Moulijn J A & Mul G, *Catal Lett*, 129 (2009) 12.

22 Carneiro J T, Savenije T J, Moulijn J A & Mul G, *J Phys Chem C,* 115 (2011) 2211.
23 Xiao-Hong Xia, Zhi-Jie Jia, Ying Yu, Ying Liang, Zhuo Wang & Li-Li Ma, *Carbon,* 45 (2007) 717.
24 Agrios A G, Gray K A & Weitz E, *Langmuir,* 19 (2003) 1402; *Langmuir,* 20 (2004) 5911.
25 Koci K, Obalova L, Matejova L, Placha D, Lancy Z, Jirkovsky J & Solcova O, *Appl Catal B Environ,* 89 (2009) 494.
26 Spurr R A & Myers H, *Analy Chem,* 29 (1957) 760.
27 Mizuno T, Adachi K, Ohta K & Saji A, *J Photochem Photobiol A: Chem,* 98 (1996) 87.
28 Subrahmanyam M, Kaneco S & Alonso-Vante N, *Appl Catal B: Environ,* 23 (1999) 169.
29 Tanaka K, Kumagai H, Hattori H, Kudo M & Hasagawa S, *J Catal*, 127 (1991) 221.
30 Carneiro J T, Chieh-Chao Yang, Moulijn J A & Mul G, *J Catal*, 277 (2011) 129.
31 Asi M A, He C, Su M, Xia D, Lin L, Deng H, Xiong Y, Qiu R & Li X, *Catal Today,* doi:10.1016/j.cattod.2011.02.055.
32 Anpo M, Yamashita H, Ichihashi Y & Ehara S, *J Electroanal Chem*, 396 (1995) 21.
33 Yang C, Yu Y, van der Linden B, Wu J C S & Mul G, *J Am Chem Soc,* 132 (2010) 8398.
34 Dimitrijevic N M, Vijayan B K, Poluektov O G, Raijh T, Gray K A, He H & Zapol P, *J Am Chem Soc,*133 (2011) 3964.
35 Ying Li, Wang W, Zhan Z, Woo M, Wu C & Biswas P, *Appl Catal B: Environ,* 100(2010) 386; Tan S S, Zou L, Hu E, *Sci & Technol Adv Mat,* 8 (2007) 89; Lin W Y, Han H X & Frei H, *J Phys Chem B,* 108 (2004) 18269.
36 Wu J C S, *Catal Surv Asia*, 13 (2009) 30.
37 Sasirekha N, Basha S J S & Shanthi K, *Appl Catal B: Environ*, 62 (2006) 169.
38 Dey G R, Belapurkar A D & Kishore K, *J Photochem Photobiol A: Chem,* 163 (2004) 503.
39 Kočí K, Obalová L & Šolcová O, *Chem Process Eng*, 31 (2010) 395.
40 Tan S S, Zou L & Hu E, *Catal Today,* 131 (2008) 125.
41 Hussain S T, Khan K & Hussain R, *J Nat Gas Chem,* 18 (2009) 383.
42 Liu Y, Huang B, Dai Y, Zhang X, Qin X, Jiang M & Whangbo M, *Catal Comm,* 11 (2009) 210.
43 Adachi K, Ohta K & Mizuno T, *Solar Energy,* 53 (1994) 187.
44 Lo C C, Hung C H, Yuan C S & Wu J F, *Solar Energy Mater Sol Cells,* 91 (2007) 1765.
45 Hoffmann M R, Moss J A & Baum M M, *Dalton Trans,* 40 (2011) 5151.
46 Kim K S, Barteau M A & Farneth W E, *Langmuir,* 4 (1988) 533.
47 Jones P & Hockey J A, *Trans Faraday Soc*, 67 (1971) 2769.
48 Lusvardi V S, Barteau M A & Farneth W E, *J Catal,* 153 (1995) 41.
49 Tanaka K & White J M, *J Phys Chem,* 86 (1982) 4708.
50 Kim K S & Barteau M A, *Surf Sci,* 223 (1989) 13.
51 Kim K S & Barteau M A, *J Mol Catal,* 63 (1990) 103s.
52 Kim K S & Barteau M A, *Langmuir,* 4 (1988) 945.
53 Jones P & Hockey J A, *Trans Faraday Soc,* 67 (1971) 2679.
54 Li K, Martin D & Tang J, *Chinese J Catal*, 32 (2011) 879.
55 Hussein G A M, Sheppard N, Zaki M I & Fahim R B, *J Chem Soc Faraday Trans*, 85 (1989) 1723; 87 (1991) 2655; 2661.